

Extended measurement of the proton spectrum with CALET on the International Space Station

Kazuyoshi Kobayashi^{a,b,*} and P. S. Marrocchesi^{c,d} on behalf of the CALET

Collaboration

(a complete list of authors can be found at the end of the proceedings)

^aWaseda Research Institute of Science and Engineering, Waseda University, 17 Kikuicho, Shinjuku, Tokyo 162-0044, Japan

^bJEM Utilization Center, Human Spaceflight Technology Directorate, Japan Aerospace Exploration Agency, 2-1-1 Sengen, Tsukuba, Ibaraki 305-8505, Japan

^cDept. of Physical Sciences, Earth and Environment, Univ. of Siena, 53100 Siena, Italy

^dINFN Sezione di Pisa, Polo Fibonacci, Largo B. Pontecorvo, 3-56127 Pisa, Italy

E-mail: kenkou@aoni.waseda.jp, marrocchesi@pi.infn.it

Calorimetric Electron Telescope (CALET) is aiming to measure the main components of high energy cosmic rays up to 1 PeV in order to understand the cosmic ray acceleration and propagation. The detector consisting of a charge detector, an imaging calorimeter, and a total absorption calorimeter, is located on the International Space Station. The thickness of the calorimeter corresponds to 30 radiation length and to 1.3 proton interaction length. Data taking has started in October 2015 and continues stably without any serious troubles. We have taken data for more than 5 years so far. We present the latest result of proton spectrum analysis in the energy region from 50 GeV to 60 TeV. A fiducial geometrical factor of 510 cm² sr is used. The energy resolution of proton is 30-40%. The remaining background is less than 10% in 50 GeV < E < 10 TeV region. Compared to our previous result published in Physical Review Letters in 2019, more than two years of data has been increased. Spectral hardening around 500 GeV is then confirmed with higher statistics. We newly observed spectral softening above 10 TeV.

37th International Cosmic Ray Conference (ICRC 2021)

July 12th – 23rd, 2021

Online – Berlin, Germany

*Presenter

1. Introduction

Direct measurements of cosmic-ray nuclei up to the PeV energy scale provide various insight into the general phenomenology of cosmic-ray acceleration and propagation in the Galaxy. A possible charge-dependent cutoff in the nuclei spectra is hypothesized to explain in the all-nuclei spectrum. The spectral hardening in the various nuclei has been observed around hundreds of GeV per nucleon energy region. In case of proton, we have reported the hardening with much higher statistics than previous experiments [1] [2]. In addition, DAMPE recently reported that proton spectral softening in the energy region over 1 TeV [3]. It is crucial to observe both the spectral hardening and the softening precisely in order to determine the mechanism of cosmic-ray acceleration and propagation in the Galaxy.

2. CALET detector

The CALorimetric Electron Telescope (CALET) [4], a space-based instrument optimized for the measurement of the all-electron spectrum [5, 6] and equipped with a fully active calorimeter, can also measure the various cosmic-ray nuclei including proton in the energy range up to 1 PeV. The thickness of the calorimeter corresponds to 30 radiation length (at normal incidence) and to 1.3 proton interaction length.

The CALET detector consists of a charge detector (CHD), a 3 radiation-length thick imaging calorimeter (IMC) and a 27 radiation-length thick total absorption calorimeter (TASC), with a field of view of 45° from zenith. A fiducial geometrical factor of approximate $510 \text{ cm}^2 \text{ sr}$ for particles penetrating CHD top to TASC bottom, with 2 cm margins at the first and the last TASC layers (acceptance A), and corresponding to about 40% of the total acceptance [6], is used in this analysis. The CHD, which identifies the charge of the incident particle, is comprised of a pair of plastic scintillator hodoscopes arranged in two orthogonal layers. The IMC is a sampling calorimeter alternating thin layers of Tungsten absorber with layers of scintillating fibers readout individually, also providing an independent charge measurement via multiple dE/dx samples. The TASC is a tightly packed lead-tungstate (PbWO_4) hodoscope, measuring the energy of showering particles in the detector. More than 6 orders of magnitude is covered by four different gain ranges. Due to the wide dynamic range in a single instrument, we can study the detailed shape of the spectrum without large systematic uncertainties from different detectors. Detailed description of the instrument is given in the Supplemental Material of Ref. [5].

The instrument was launched on August 19, 2015 and emplaced on the Japanese Experiment Module-Exposed Facility (JEM-EF) on the International Space Station (ISS) with an expected mission duration of five years. Now the mission was extended and the duration is expected to nine years (or more) in total. Figure 1 show the ISS and a schematic view of the CALET detector. Scientific observations started on October 13, 2015 and the detector operation continues without any serious troubles so far.

3. Analysis

We have analyzed flight data collected for 1815 days from October 13, 2015 to September 30, 2020. The total observation livetime for the HE shower trigger [4] is 1539 days and livetime

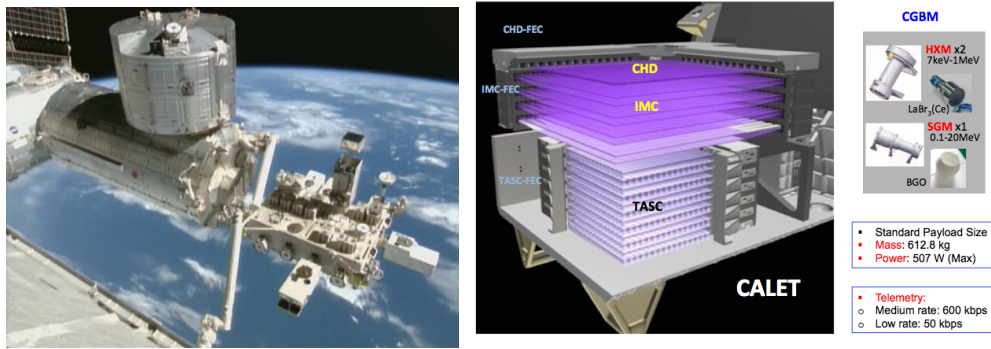


Figure 1: CALET detector. Left figure shows the ISS. The right edge is the JEM-EF and the CALET is in that area. Right figure shows a schematic view of the CALET detector.

fraction to total time is 84%. In addition, the low-energy (LE) shower trigger operated at a high geomagnetic latitude [4] is used to extend the energy coverage toward the lower energy region. In spite of a limited livetime of 27.9 days, LE data provide sufficient statistics for protons below a few hundred GeV. Monte Carlo (MC) simulations, reproducing the detailed detector configuration, physics processes, as well as detector signals, are based on the EPICS simulation package [8].

3.1 Event selection

In order to obtain the proton event sample, we apply the following selection criteria: we required that (1) In the energy range of $E > 300$ GeV, HE trigger should be issued and the energy deposit sum of IMC 7th and 8th layers should be more than 5 MIP in X and Y view, individually. Also the energy deposit of TASC 1st layer should be more than 10 MIP. In the energy range of $E < 300$ GeV, LE trigger should be issued and the energy deposit sum of IMC 7th and 8th layers should be more than 5 MIP in X and Y view, individually. Also the energy deposit of TASC 1st layer should be more than 100 MIP. (2) Acceptance A is required in the hit geometrical condition. (3) Kalman filter (KF) tracking in IMC should be succeeded both in X and Y view. (4) Energy deposit inside the Moliere radius along the KF track in IMC should be less than 70% of total energy deposit. (5) Off-acceptance events should be removed by the following two methods. One is that maximum fractional energy deposit in TASC layer should be less than 0.4. The other is that maximum energy deposit ratio of the edge channels to the maximum channels in each layer should be less than 0.4. (6) Center of gravity of TASC energy deposit in X1 and Y1 layer should be consistent with the IMC track. (7) Shower start in IMC is required. (8) Charge is identified as proton using both CHD and IMC energy deposits. Charge (Z) is calculated from $Z = a(E) \sqrt{N}^{b(E)}$, where N is the energy deposit in MIP and $a(E)$ and $b(E)$ are energy dependent parameters determined using MC simulation so that the Z should be 1 for proton and 2 for helium. The selection criteria is determined to keep the efficiency is 95% for lower Z side and 98% for higher Z side. Criterion (4) is required to remove electron background. Criterion (5) remove the particle coming from the side of the detector. Criterion (6) remove the mis-reconstructed events.

3.2 Background

Background is estimated with MC simulations from cosmic ray protons, helium and electrons. After applying all the event selection, the dominant background comes from the off-acceptance protons in $E < 5$ TeV. In $E > 5$ TeV, helium is the main background source.

Figure 2 shows a proton candidate with energy deposit of 2.9 TeV in the detector. The event example demonstrates s capability to reconstruct and identify high energy protons. Because of the limited energy resolution (30-40%), energy unfolding is required to estimate the primary energy distribution. It is important, therefore, to infer the detector response at the highest energies covered by the analysis. First, we make response matrix between true and observed energy spectrum using MC simulation. Then, we apply unfolding iteratively based on Bayes theorem with helium and electron background consideration.

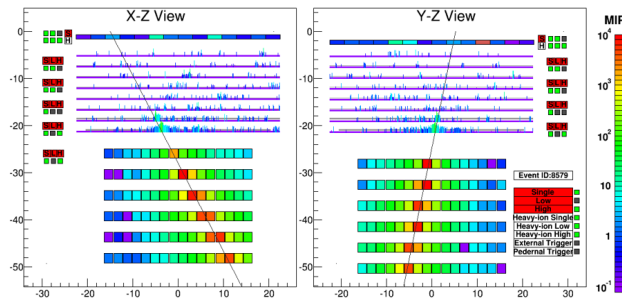


Figure 2: Proton event display with 2.9 TeV energy deposit.

3.3 Systematic uncertainty

There are two components we take into account as systematic uncertainties. One is the energy independent component, which is 4.1% in total. It contains the uncertainties of livetime (3.4]%), radiation environment (1.8%), and long-term stability (1.4%). The other is the energy dependent component, that is less than 10% in $E < 10$ TeV. We take into account the uncertainties of MC model dependence, IMC track consistency with TASC, shower start in IMC, charge identification, energy unfolding, beam test configuration. In $E > 10$ TeV, especially the uncertainties of MC model dependence and charge identification becomes larger. In $10 < E < 60$ TeV the uncertainty is 30% at maximum.

3.4 Proton spectrum

The proton spectrum ($\Phi(E)$) is obtained from the following equation:

$$\Phi(E) = \frac{N(E)}{S\Omega T \Delta E \epsilon(E)} \quad (1)$$

, where $N(E)$ is the number of selected events in $E = E + \Delta E$, $S\Omega$ is the geometrical acceptance ($510\text{cm}^2\text{sr}$), T is livetime (1539 days for HE and 27.9 days for LE, respectively), ΔE is the energy bin width, and $\epsilon(E)$ is the detection efficiency. Figure 3 shows the proton spectrum in the energy region

from 30 GeV to 60 TeV, compared with AMS-02, CREAM-III, and DAMPE. In the low energy region of $E < 200$ GeV, the result is fully consistent. In the higher energy region, the systematic difference is observed, but the difference is within the uncertainty. We confirmed the spectral hardening around 500 GeV reported in [7]. We also observed a spectral softening in $E > 10$ TeV. We have tested two independent analyses with different efficiencies. We confirmed that the two results are consistent.

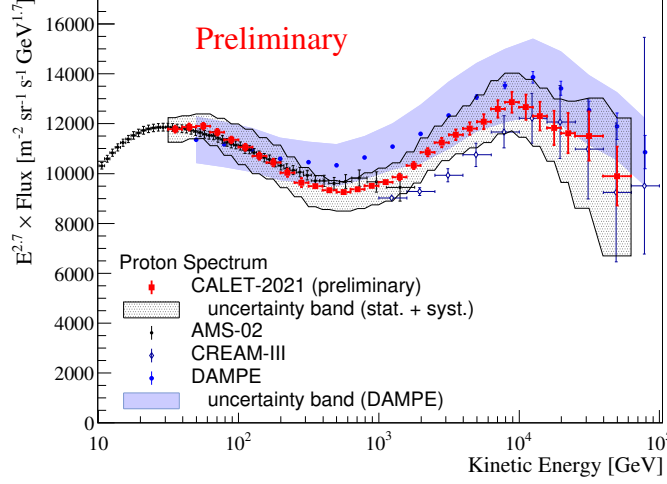


Figure 3: Proton spectrum measured by CALET (red circles) compared to the experimental results of AMS02 [1], CREAM-III [2], and DAMPE [3]. Hatched band shows the total uncertainty for CALET. Dark blue colored band shows the total uncertainty for DAMPE.

3.5 Discussion

In order to calculate the hardening and softening quantitatively, we apply spectral fitting to the proton spectrum using double broken power law function defined as follows:

$$\Phi = E^{2.7} \times C \times \left(1 - \frac{p_0}{E} - \frac{p_1}{E^2}\right) \times \left(\frac{E}{45}\right)^\gamma \times \left(1 + \left(\frac{E}{E_0}\right)^S\right)^{\frac{\Delta\gamma}{S}} \times \left(1 + \left(\frac{E}{E_1}\right)^S\right)^{\frac{\Delta\gamma_1}{S}} \quad (2)$$

, where Φ is the proton flux $\times E^{2.7}$, C is the normalization factor, p_0 and p_1 is the fitting parameter for the low energy region, S is the smoothness parameter, γ is the spectral index, $\Delta\gamma$ is the spectral index for hardening, E_0 is the hardening start energy, $\Delta\gamma_1$ is the spectral index for softening, E_1 is the softening start energy.

In figure 4, black circles show the data with statistical errors and red line shows the best fitted function. χ^2 is 2.9 in 22 degree of freedom. The best fitted parameters are as follows: $p_0 = 9.1 \pm 26$, $p_1 = -6.6 \pm 470$, $\gamma = -2.9 \pm 0.3$, $S = 2.1 \pm 2.0$, $\Delta\gamma = (4.4 \pm 3.8) \times 10^{-1}$, $E_0 = (5.5 \pm 1.3) \times 10^2$ GeV, $\Delta\gamma_1 = (-4.4 \pm 3.0) \times 10^{-1}$, and $E_1 = (1.1 \pm 0.4) \times 10^4$ GeV. The hardening starts at 550 ± 130 GeV and the softening starts at 11 ± 4 TeV.

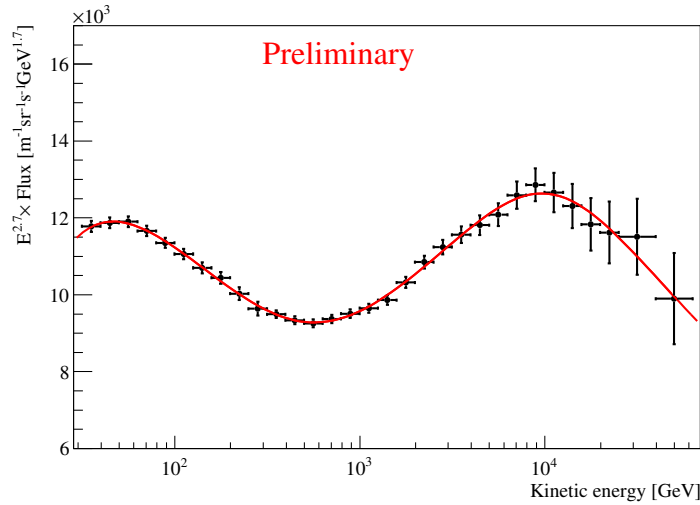


Figure 4: CALET Proton spectrum fitted with the function in Equation 2.

4. Summary

We have performed extended measurement of proton spectrum with CALET data taken from Oct. 2015 to Sep. 2020. We have increased two more years of statistics since we published in 2019. We confirmed the spectral hardening around 500 GeV. Also the energy region is expanded to 60 TeV and then observed spectral softening in $E > 10$ TeV region.

References

- [1] M. Aguilar *et al.* (AMS Collaboration), *Phys. Rev. Lett.* **114**, 171103 (2015).
- [2] Y. S. Yoon *et al.* (CREAM-III Collaboration), *Astrophys. J* **839**, 5 (2017).
- [3] Q. An *et al.* (DAMPE Collaboration), *Science Adv.* 2019, 5, eaax3793.
- [4] Y. Asaoka *et al.* (CALET Collaboration), *Astropart. Phys.* **100**, 29 (2018).
- [5] O. Adriani *et al.* (CALET Collaboration), *Phys. Rev. Lett.* **119**, 181101 (2017).
- [6] O. Adriani *et al.* (CALET Collaboration), *Phys. Rev. Lett.* **120**, 261102 (2018).
- [7] O. Adriani *et al.* (CALET Collaboration), *Phys. Rev. Lett.* **122**, 181102 (2019).
- [8] K. Kasahara, in *Proceedings of 24th International Cosmic Ray Conference, Rome, Italy*, edited by N. Iucci and E. Lamanna (International Union of Pure and Applied Physics, 1995) Vol. 1, p. 399, <http://adsabs.harvard.edu/full/1995ICRC....1..399K>.

Full Authors List: CALET Collaboration

O. Adriani^{1,2}, Y. Akaike^{3,4}, K. Asano⁵, Y. Asaoka⁵, E. Berti^{1,2}, G. Bigongiari^{6,7}, W. R. Binns⁸, M. Bongi^{1,2}, P. Brogi^{6,7}, A. Bruno^{9,10}, J. H. Buckley⁸, N. Cannady^{11,12,13}, G. Castellini¹⁴, C. Checchia⁶, M. L. Cherry¹⁵, G. Collazuol^{16,17}, K. Ebisawa¹⁸, A. W. Ficklin¹⁵, H. Fuke¹⁸, S. Gonzi^{1,2}, T. G. Guzik¹⁵, T. Hams¹¹, K. Hibino¹⁹, M. Ichimura²⁰, K. Ioka²¹, W. Ishizaki⁵, M. H. Israel⁸, K. Kasahara²², J. Kataoka²³, R. Kataoka²⁴, Y. Katayose²⁵, C. Kato²⁶, N. Kawanaka^{27,28}, Y. Kawakubo¹⁵, K. Kobayashi^{3,4}, K. Kohri²⁹, H. S. Krawczynski⁸, J. F. Krizmanic^{11,12,13}, J. Link^{11,12,13}, P. Maestro^{6,7}, P. S. Marrocchesi^{6,7}, A. M. Messineo^{30,7}, J. W. Mitchell¹², S. Miyake³², A. A. Moiseev^{33,12,13}, M. Mori³⁴, N. Mori², H. M. Motz³⁵, K. Munakata²⁶, S. Nakahira¹⁸, J. Nishimura¹⁸, G. A. de Nolfo⁹, S. Okuno¹⁹, J. F. Ormes³⁶, N. Ospina^{16,17}, S. Ozawa³⁷, L. Pacini^{1,14,2}, P. Papini², B. F. Rauch⁸, S. B. Ricciarini^{14,2}, K. Sakai^{11,12,13}, T. Sakamoto³⁸, M. Sasaki^{33,12,13}, Y. Shimizu¹⁹, A. Shiomi³⁹, P. Spillantini¹, F. Stolzi^{6,7}, S. Sugita³⁸, A. Sulaj^{6,7}, M. Takita⁵, T. Tamura¹⁹, T. Terasawa⁴⁰, S. Torii³, Y. Tsunesada⁴¹, Y. Uchihori⁴², E. Vannuccini², J. P. Wefel¹⁵, K. Yamaoka⁴³, S. Yanagita⁴⁴, A. Yoshida³⁸, K. Yoshida²², and W. V. Zober⁸

¹Department of Physics, University of Florence, Via Sansone, 1, 50019 Sesto, Fiorentino, Italy, ²INFN Sezione di Florence, Via Sansone, 1, 50019 Sesto, Fiorentino, Italy, ³Waseda Research Institute for Science and Engineering, Waseda University, 17 Kikuicho, Shinjuku, Tokyo 162-0044, Japan, ⁴JEM Utilization Center, Human Spaceflight Technology Directorate, Japan Aerospace Exploration Agency, 2-1-1 Sengen, Tsukuba, Ibaraki 305-8505, Japan, ⁵Institute for Cosmic Ray Research, The University of Tokyo, 5-1-5 Kashiwa-no-Ha, Kashiwa, Chiba 277-8582, Japan, ⁶Department of Physical Sciences, Earth and Environment, University of Siena, via Roma 56, 53100 Siena, Italy, ⁷INFN Sezione di Pisa, Polo Fibonacci, Largo B. Pontecorvo, 3, 56127 Pisa, Italy, ⁸Department of Physics and McDonnell Center for the Space Sciences, Washington University, One Brookings Drive, St. Louis, Missouri 63130-4899, USA, ⁹Heliospheric Physics Laboratory, NASA/GSFC, Greenbelt, Maryland 20771, USA, ¹⁰Department of Physics, Catholic University of America, Washington, DC 20064, USA, ¹¹Center for Space Sciences and Technology, University of Maryland, Baltimore County, 1000 Hilltop Circle, Baltimore, Maryland 21250, USA, ¹²Astroparticle Physics Laboratory, NASA/GSFC, Greenbelt, Maryland 20771, USA, ¹³Center for Research and Exploration in Space Sciences and Technology, NASA/GSFC, Greenbelt, Maryland 20771, USA, ¹⁴Institute of Applied Physics (IFAC), National Research Council (CNR), Via Madonna del Piano, 10, 50019 Sesto, Fiorentino, Italy, ¹⁵Department of Physics and Astronomy, Louisiana State University, 202 Nicholson Hall, Baton Rouge, Louisiana 70803, USA, ¹⁶Department of Physics and Astronomy, University of Padova, Via Marzolo, 8, 35131 Padova, Italy, ¹⁷INFN Sezione di Padova, Via Marzolo, 8, 35131 Padova, Italy, ¹⁸Institute of Space and Astronautical Science, Japan Aerospace Exploration Agency, 3-1-1 Yoshinodai, Chuo, Sagamihara, Kanagawa 252-5210, Japan, ¹⁹Kanagawa University, 3-27-1 Rokkakubashi, Kanagawa, Yokohama, Kanagawa 221-8686, Japan, ²⁰Faculty of Science and Technology, Graduate School of Science and Technology, Hirosaki University, 3, Bunkyo, Hirosaki, Aomori 036-8561, Japan, ²¹Yukawa Institute for Theoretical Physics, Kyoto University, Kitashirakawa Oiwakecho, Sakyo, Kyoto 606-8502, Japan, ²²Department of Electronic Information Systems, Shibaura Institute of Technology, 307 Fukasaku, Minuma, Saitama 337-8570, Japan, ²³School of Advanced Science and Engineering, Waseda University, 3-4-1 Okubo, Shinjuku, Tokyo 169-8555, Japan, ²⁴National Institute of Polar Research, 10-3, Midori-cho, Tachikawa, Tokyo 190-8518, Japan, ²⁵Faculty of Engineering, Division of Intelligent Systems Engineering, Yokohama National University, 79-5 Tokiwadai, Hodogaya, Yokohama 240-8501, Japan, ²⁶Faculty of Science, Shinshu University, 3-1-1 Asahi, Matsumoto, Nagano 390-8621, Japan, ²⁷Hakubi Center, Kyoto University, Yoshida Honmachi, Sakyo-ku, Kyoto 606-8501, Japan, ²⁸Department of Astronomy, Graduate School of Science, Kyoto University, Kitashirakawa Oiwake-cho, Sakyo-ku, Kyoto 606-8502, Japan, ²⁹Institute of Particle and Nuclear Studies, High Energy Accelerator Research Organization, 1-1 Oho, Tsukuba, Ibaraki 305-0801, Japan, ³⁰University of Pisa, Polo Fibonacci, Largo B. Pontecorvo, 3, 56127 Pisa, Italy, ³¹Astroparticle Physics Laboratory, NASA/GSFC, Greenbelt, Maryland 20771, USA, ³²Department of Electrical and Electronic Systems Engineering, National Institute of Technology, Ibaraki College, 866 Nakane, Hitachinaka, Ibaraki 312-8508, Japan, ³³Department of Astronomy, University of Maryland, College Park, Maryland 20742, USA, ³⁴Department of Physical Sciences, College of Science and Engineering, Ritsumeikan University, Shiga 525-8577, Japan, ³⁵Faculty of Science and Engineering, Global Center for Science and Engineering, Waseda University, 3-4-1 Okubo, Shinjuku, Tokyo 169-8555, Japan, ³⁶Department of Physics and Astronomy, University of Denver, Physics Building, Room 211, 2112 East Wesley Avenue, Denver, Colorado 80208-6900, USA, ³⁷Quantum ICT Advanced Development Center, National Institute of Information and Communications Technology, 4-2-1 Nukui-Kitamachi, Koganei, Tokyo 184-8795, Japan, ³⁸College of Science and Engineering, Department of Physics and Mathematics, Aoyama Gakuin University, 5-10-1 Fuchinobe, Chuo, Sagamihara, Kanagawa 252-5258, Japan, ³⁹College of Industrial Technology, Nihon University, 1-2-1 Izumi, Narashino, Chiba 275-8575, Japan, ⁴⁰RIKEN, 2-1 Hirosawa, Wako, Saitama 351-0198, Japan, ⁴¹Division of Mathematics and Physics, Graduate School of Science, Osaka City University, 3-3-138 Sugimoto, Sumiyoshi, Osaka 558-8585, Japan, ⁴²National Institutes for Quantum and Radiation Science and Technology, 4-9-1 Anagawa, Inage, Chiba 263-8555, Japan, ⁴³Nagoya University, Furo, Chikusa, Nagoya 464-8601, Japan, ⁴⁴College of Science, Ibaraki University, 2-1-1 Bunkyo, Mito, Ibaraki 310-8512, Japan